

23p

X-64 11260⁸
N65-89028

Code 2 A

(NASA TMX-51368)

CLOUD HEIGHTS AND NIGHTTIME CLOUD COVER
FROM TIROS RADIATION DATA

[S. I. Rasool] [1963] 23p ref

Goddard Institute for Space Studies, New York, N.Y.
National Aeronautics and Space Administration,
New York, New York

Submitted for Publication

Submitted to Journal of Atmospheric Sciences, November, 1963

Available to NASA Offices and

NASA Centers Only

In a recent paper, Arking (1963) has derived the global distribution of cloud cover by the analysis of TIROS III video pictures. In Fig. 7 (Curve 1) is plotted the latitudinal distribution of average daytime percentage cloud cover as obtained by Arking for the period of July 12, through September 10, 1961.

In the present study we attempt, using these data and the simultaneous radiation measurements by TIROS III, to derive the average latitudinal distribution of cloud top heights and thence the nighttime cloud cover. Curve 2 in Fig. 7 shows the resulting percentage cloud cover during the night as a function of latitude.

TIROS INFRA-RED DATA

The radiation instrumentation in TIROS and the physical significance of this experiment have already been described by several authors (Bandein et al., 1961, Nordberg et al., 1962).

Three of the five channels of the TIROS radiometer measure terrestrial radiation in the far infra-red corresponding to wavelengths between $5.8 - 6.5 \mu$, $8 - 12 \mu$, and $7 - 30 \mu$. The other two channels record the solar radiation in the visible, as reflected

by the earth, to obtain an estimate of the albedo of any region. The wavelengths of the infra-red channels have been chosen so as to provide information on the temperature at different levels of the atmosphere and to give an estimate of the total outgoing radiation in the infra-red.

In this discussion we shall only be concerned with Channel 2, sensitive in the 8 - 12 μ region of the infra-red.

The main absorber of infra-red radiation in the earth's atmosphere is water vapor. The absorption coefficient, however, varies considerably with wavelength between 4 and 50 μ , where almost all the energy of the terrestrial radiation is confined.

In the 8 - 12 μ spectral interval the absorption by water vapor and also by CO₂, the other important absorber of the infra-red radiation, is at its minimum. Consequently, in the absence of clouds, Channel 2 of the satellite radiometer, measuring in this atmospheric "window," records energy originating from very near the ground corresponding to an effective temperature only ~ 5 - 10 °K less than the ground temperature (Wark, Yamamoto, Lienesch, 1962, Prabhakara and Rasool, 1963).

Reasonably thick clouds, however, are practically opaque to infra-red radiation of wavelengths $> 4 \mu$ (Shiffirin 1961). As there is very little water vapor above, and assuming that the albedo of the clouds in the far infra-red is negligible, the radiometer in the presence of thick clouds will record energy corresponding to the cloud top temperature. This may be as much as 40 - 50 °K lower than the surface temperature.

If, therefore, for any given instant, both the TIROS measured temperatures in this "window" channel and the actual surface temperatures are available, then knowing the lapse rate in the atmosphere, a quick estimate of cloud height can be obtained. On the other hand, on a climatological basis, if the satellite-measured temperatures for a given region are averaged over a season, then the departure of this temperature from the observed ground temperature will be mainly dependent on three variables -- cloud amount, cloud height, and water vapor distribution in the atmosphere.

As mentioned earlier, the effect of water vapor is comparatively small, and from our knowledge of climatological distribution of the water vapor over the globe, its effect on the temperatures

can be accounted for.

The strong effect of clouds on the TIROS III measured temperatures in the "window" channel is demonstrated by Figure 1.

In this figure are plotted the regional and temporal averages of the temperatures measured by Channel 2 of TIROS III during daytime (0600 - 1800 hours Local Time) for the period of July 12, through September 10, 1961. The inclination of the TIROS orbit being $\sim 48^\circ$, the measurements for the polar regions are not available.

The surface of the earth between 50° N and 50° S has been divided into 10° latitude X 10° longitude grid, and all measurements taken by the satellite in each grid at nadir angle $< 25^\circ$ and between local time 0600 and 1800 hours have been averaged for the period mentioned above. In most cases there are > 500 observation points per grid.

The very dark shades correspond to high radiation intensities with effective temperatures ranging above 290°K . The lightest shades correspond to temperatures of the order of 240°K . The two

triangular areas, which are diagonally opposite and comprise a part of South America and Southern Siberia, have been left blank because of the unavailability of the telemetry from the TIROS for these regions.

Several interesting features are revealed by examining this figure. (1) The relatively cold temperature belt near the equator probably corresponds to the high cloudiness usually observed in the equatorial region. (2) The subtropical belt in each of the hemispheres show relatively higher temperatures and, therefore, probably less clouds than in the equatorial regions. (3) Extremely low temperatures measured over East Pakistan and India imply a heavy cloud cover over these regions which is, in all probability, the monsoon activity in this season. An almost quasi-permanent cloud cover over central Africa is also indicated from this diagram.

This is supported by comparing Figure 1 with Figure 2 in which are plotted the global distribution of cloud cover, also in a 10° X 10° grid taken from the climatological estimates of Haurwitz and Austin (1944). In figure 2, the darkest shades correspond to 20% cloudiness, and the lightest to 70% cloudiness. The agreement

in the main features of the two figures is striking, except that the TIROS III measured extremely high temperatures over South Pacific indicating a relatively clear area, while the climatology had ignored it.

DEDUCTION OF CLOUD HEIGHTS AND CLOUD COVER

Although it is interesting to note the resemblance between figures 1 and 2, the actual derivation of cloud amounts from the TIROS radiation data is fairly involved.

As mentioned earlier, several factors, viz, cloud amount, cloud height, surface temperature, vertical distribution of water vapor and of temperature, influence the 'effective' temperatures measured by the satellite. By the method described below we have, however, attempted to separate the effect of these parameters in order to obtain a reasonable estimate of cloud height from TIROS radiation data.

Using the climatological estimates of the global distribution of surface temperature (Haurwitz and Austin, 1944), the latitudinal variations in the vertical distribution of temperature (Davis, 1962,

London, 1957), the total amounts of water vapor and ozone and their vertical distributions, we have constructed ten different model atmospheres which correspond to the ten latitudinal belts between 50° N and 50° S for the months of July and August.

The radiation flux in the $8 - 12 \mu$ region, which would be emitted from such atmospheres, was then calculated following a method described in an earlier paper (Prabhakara and Rasool, 1963). The flux values thus calculated give the black body temperatures TIROS will observe above these atmospheres if the atmosphere were completely cloudless. Similar calculations were then repeated assuming the presence of thick clouds at various altitudes and of varying proportions. The clouds are assumed to be completely opaque to the far infra-red and the radiation is emitted only from the top of the cloud.

In Figures 3 and 4 the results obtained for two such model atmospheres are shown. The family of five curves show the difference (ΔT) between the surface temperature and the effective black body temperature observed by the satellite in the presence of different amounts of clouds located at altitudes of 2, 3, 4, 5, or 6 kms.

The intersection point of these curves with the ordinate in Figure 3 is at 12.5°K . This indicates that in a hot and humid atmosphere, even in complete absence of clouds, the satellite would observe an effective temperature about 12°K lower than the surface temperature. In Figure 4 is shown another extreme case, this time of a dry and cold atmosphere where the ΔT , in the absence of clouds, is only 4°K .

If, therefore, for any given region, one has an estimate of surface temperature, the amount of water vapor in the atmosphere and of the percentage cloud cover, then with such a family of curves, combined with the TIROS radiation data of the "window" channel, one can derive an approximate value for the effective height of the cloud tops.

In order to determine the latitudinal distribution of the effective cloud heights for the months of July and August 1961, we calculate the following parameters for each 10° latitudinal belt between 50°N and 50°S .

The satellite-observed temperatures in the "window" channel

are averaged separately for day and for night for the period July 12 through September 10, 1961.

The latitudinal means of day and night surface temperatures for the same period were determined from the Monthly Climatic Data of the World (U.S. Weather Bureau); supplementing these data by climatological estimates of Haurwitz and Austin (1944) for the oceanic regions.

The difference (ΔT) between the mean surface temperatures and the average effective temperatures measured by the TIROS Channel 2 in each latitudinal belt is plotted in Figure 5 separately for day and for night.

Latitudinal averages of daytime percentage cloud cover for the same period given by Arking (1963) are shown in Figure 7 (curve 1).

Now with both the ΔT and percentage cloud cover being known for daytime, we can use our nomograms (e.g. figs. 3 and 4) to determine the average daytime cloud height for each latitudinal belt. The heights thus deduced are plotted as a function of latitude

in Figure 6.

If we assume that on an average, cloud heights derived from the daytime measurements are also valid for the night, we can now use the ΔT values for the night (Fig. 5) and the heights plotted in Figure 6 to determine the nighttime cloud cover as a function of latitude.

The resulting latitudinal distribution of the nighttime cloud cover is plotted as Curve 2 in Figure 7.

A comparison of the day and night curves immediately shows that in the southern hemisphere, which is largely oceanic, the percentage cloudiness is much higher at night than during the day. In the northern hemisphere, on the other hand, the nocturnal nebulosity could be as low as $\sim 20\%$ for the latitudes of 20° to 40° .

These results are based on the debatable assumption that, on an average, for a given latitudinal belt the cloud-top heights do not change from day to night. In case this assumption is not correct, our results would then indicate that, in order to have

the same amount of cloudiness for both day and night, the cloud heights in the Southern hemisphere should be 2 to 4 km higher at night than in the daytime, and lower by 1 to 3 km in the Northern hemisphere.

Similar analysis of the TIROS radiation data can also be made to determine the longitudinal as well as latitudinal distribution of nighttime cloud cover, but it requires more detailed information on the global distribution of surface temperatures and water vapor amounts and the possible variations in the emissivities of land areas (Beuttner 1963). Such calculations are in progress and will be published separately.

ACKNOWLEDGEMENT

I wish to thank Professor R. M. Goody for reading over the manuscript and making valuable comments.

REFERENCES

- | | | |
|--|------|---|
| Arking, A. | 1963 | "Global distribution of cloud cover as deduced from TIROS photographs," Space Research IV, P. Müller, ed. (North Holland Publishing Co., in press). |
| Bandeem, W.R.,
R. A. Hanel,
J. Licht, R.A.
Stampfl and W.G.
Stroud | 1961 | "Infrared and Reflected Solar Radiation Measurements from the TIROS II Meteorological Satellite," <u>J. Geophys. Res.</u> , <u>65</u> , 3165. |
| Beuttner, K.J.K.,
Kern, C.D. | 1963 | Science, Vol. 142, p. 671. |
| Davis, P. | 1961 | "A Re-examination of the Heat Budget of the Troposphere and Lower Stratosphere," <u>Scientific Report No. 3</u> , Contract No. AF 19(604)-6146, Research Division, College of Engineering, New York University. |
| Haurwitz, B., and
J. M. Austin | 1944 | <u>Climatology</u> , McGraw-Hill Book Co., Inc., New York, 410 pp. |
| London, J. | 1957 | "A Study of the atmospheric heat balance. Final Report, Contract No. AF 19(122)-165. Research Division College of Engineering, New York University. |
| Nordberg, W.,
W.R. Bandeen,
B.J. Conrath,
V. Kunde and
I. Persano | 1962 | "Preliminary Results of Radiation Measurements from the TIROS III Meteorological Satellite", <u>J. Atm. Sci.</u> <u>19</u> , 20-30. |
| Prabhakara, C., and
S. I. Rasool | 1963 | "Evaluation of TIROS Infrared Data", Proceedings of the First International Symposium on Rocket and Satellite Meteorology, H. Wexler and J. E. Caskey Jr., ed. (North-Holland Publishing Co., Amsterdam). |

- Shiffarin, K.S. 1961 "Spectral Properties of Clouds,"
Geof. Pura. Appl., vol. 48, p. 129.
- Wark, D.Q., 1962 "Methods of Estimating Infrared Flux
Yamamoto, G., and and Surface Temperature from Meteoro-
Lienesch, J.H. logical Satellites," J. Atm. Sci. 19.

FIGURE CAPTIONS

- Fig. 1. Global distribution of average temperatures measured by TIROS radiometer Channel 2 for the period July 12, through September 10, 1961. Darkest shade, $T > 295^{\circ}\text{K}$, lightest shade, $T < 255^{\circ}\text{K}$.
- Fig. 2. Global distribution of average cloud cover for July (after Haurwitz and Austin, 1944). Darkest shade -- cloud cover $> 70\%$, lightest shade -- cloud cover $< 20\%$.
- Fig. 3. ΔT as a function of percentage cloud cover with cloud tops at various altitudes. ΔT is the difference between the average surface temperature and the equivalent black body temperature measured by the TIROS III, Channel 2. A case of hot and humid atmosphere.
- Fig. 4. Same as fig. 3 -- A case of cold and dry atmosphere.
- Fig. 5. ΔT as a function of latitude -- for day and for night.
- Fig. 6. Effective cloud top heights deduced from the daytime observation of TIROS III as a function of latitude.
- Fig. 7. Curve 1. Daytime average percentage cloud cover for the period July 12, through September 10 as a function of latitude. After Arking.
- Curve 2. Nighttime average percentage cloud cover for the same period deduced from TIROS window channel data.

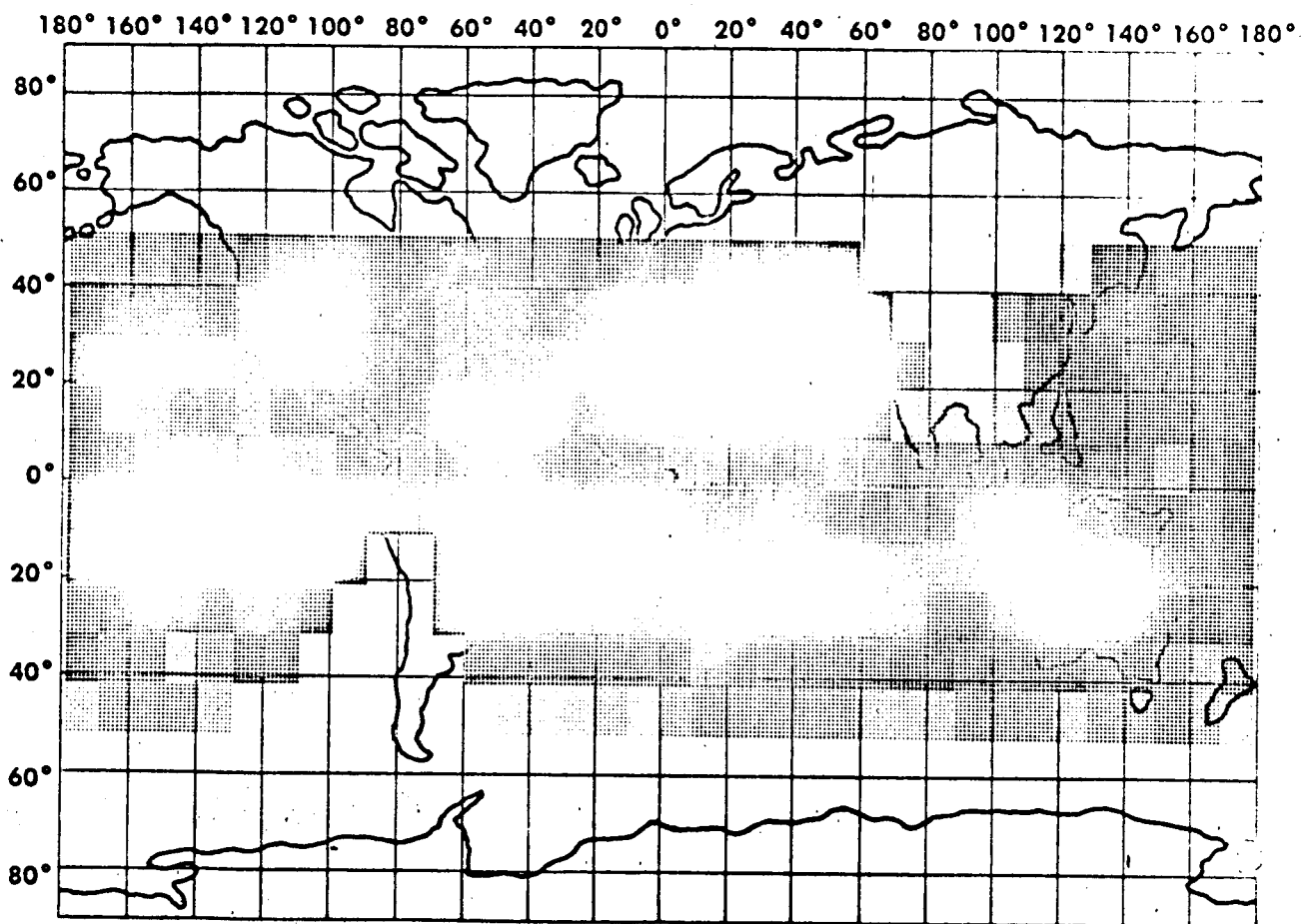


Fig. 1

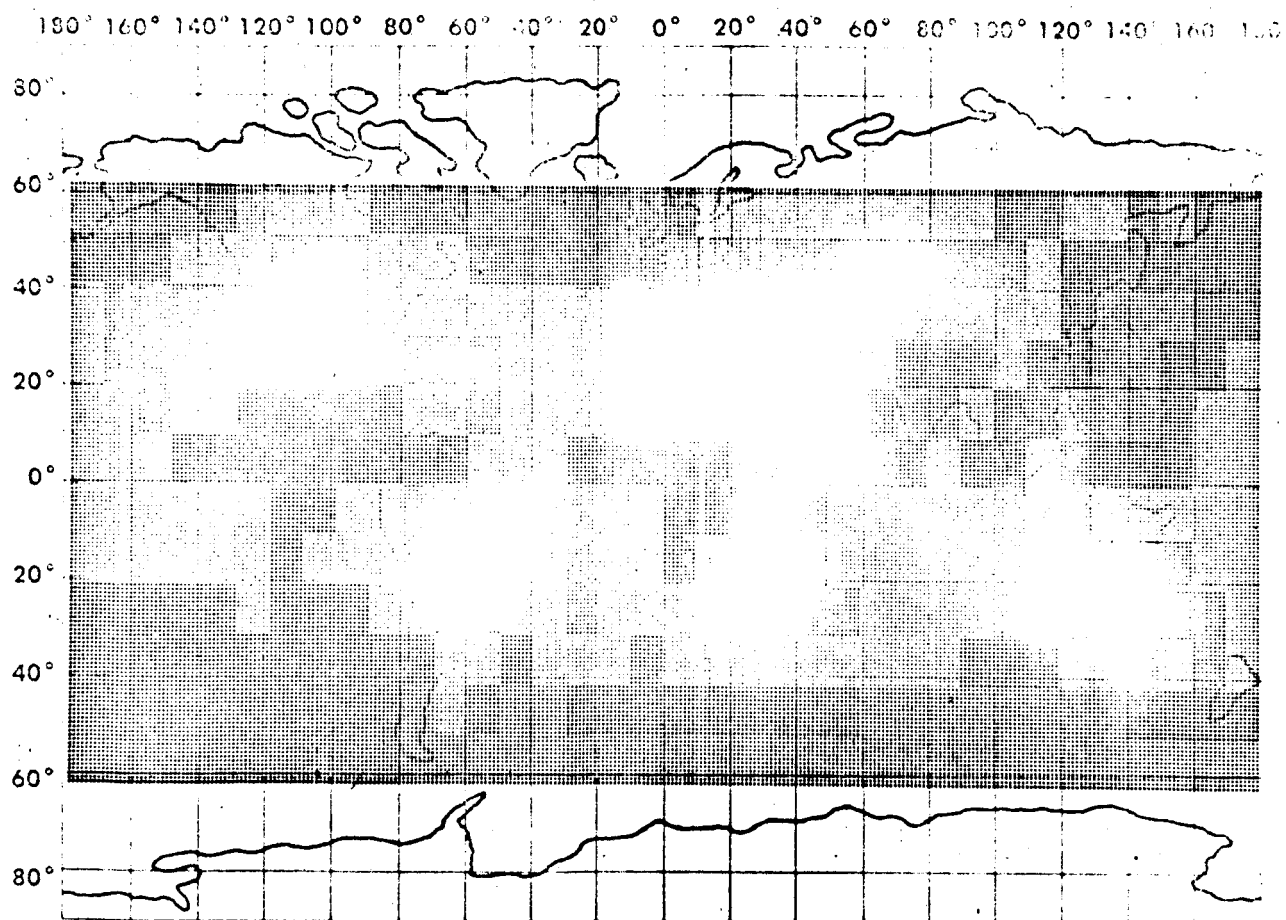


Fig. 2

